



# Microfluidic devices for measuring gene network dynamics in single cells

Matthew R. Bennett\* and Jeff Hasty†

**Abstract** | The dynamics governing gene regulation have an important role in determining the phenotype of a cell or organism. From processing extracellular signals to generating internal rhythms, gene networks are central to many time-dependent cellular processes. Recent technological advances now make it possible to track the dynamics of gene networks in single cells under various environmental conditions using microfluidic ‘lab-on-a-chip’ devices, and researchers are using these new techniques to analyse cellular dynamics and discover regulatory mechanisms. These technologies are expected to yield novel insights and allow the construction of mathematical models that more accurately describe the complex dynamics of gene regulation.

The study of gene regulation has undergone a transformation over the past decade owing to the maturation of new technologies and an increased interest in the topic among mathematical biologists. New assay techniques, particularly those involving DNA microarrays or fluorescent proteins, have allowed researchers to quantify the relative levels of gene expression in cells and test mathematical models of gene networks *in vivo*. These technologies are at the heart of two new scientific disciplines, namely ‘systems biology’ and ‘synthetic biology’, each of which takes a starkly different approach to the study of gene regulation<sup>1</sup>. Systems biologists take a top-down approach by studying entire large-scale gene networks with the goal of obtaining an integrated understanding of genomic function<sup>2–4</sup>. By contrast, synthetic biologists take a bottom-up approach by studying simplified gene networks consisting of just one or a few genes with the goal of uncovering the fundamental principles and mechanisms that govern gene regulation. The definition of synthetic biology is now very broad and includes general work on metabolic and genetic engineering. Here, we use the term to refer to the original definition: the study of gene regulation through the creation of mathematical models and simple *de novo* circuits. Although we focus on synthetic biology in this Review, systems and synthetic biology are connected by the belief that mathematical and computational modelling will lead to a better understanding of gene regulation<sup>5</sup>.

Because synthetic biologists are more concerned with the intricacies of gene regulation, their models tend to include more details of molecular dynamics

than those from systems biology. The ability to probe the dynamics of gene networks at the single-cell level is key to the synthetic biology approach. Systems-level effects that control whole genomes or even multicellular and population-scale phenomena are important, but synthetic biologists take the stance that an understanding of the mechanisms underlying gene regulation is just as important and will aid our overall understanding of phenotypic responses. To probe these small-scale interactions and mechanisms, some synthetic biology laboratories have begun using microfluidic ‘lab-on-a-chip’ devices to trap single cells or small populations of cells for long-term data acquisition. Over the past decade, microfluidic devices have been used in a myriad of studies, and their use is not limited to the analysis of single-cell or even single-species phenomena. There are many good reviews on the design and manufacture of microfluidic chips<sup>6–8</sup>, as well as on their use in biological settings<sup>9–14</sup>.

In this Review, we examine the ways in which microfluidic devices can be used to examine intracellular signalling pathways and the dynamics of gene regulation in bacteria, yeast and higher eukaryotes from the standpoint of synthetic biology. We discuss some of the various designs of microfluidic devices and the ways in which these chips can be used to create non-trivial environmental perturbations, such as time-dependent fluctuations and spatial gradients of media concentrations. The ability to control the extracellular environment has allowed researchers to interrogate cellular signalling pathways and test mathematical models of gene regulation in new ways.

\*Department of Biochemistry and Cell Biology and Institute of Biosciences and Bioengineering, Rice University, 6100 Main Street, Houston, Texas 77005-1892, USA.

†Departments of Molecular Biology and Bioengineering and BioCircuits Institute, University of California, San Diego, La Jolla, California 92093-0412, USA.

Correspondence to M.R.B. e-mail:

[matthew.bennett@rice.edu](mailto:matthew.bennett@rice.edu)  
doi:10.1038/nrg2625

Published online  
11 August 2009

We begin by discussing conventional methods for quantifying fluorescent protein expression, such as flow cytometry and fluorescence microscopy, and their advantages and disadvantages. We then introduce microfluidic devices and describe how they can be used to study gene network dynamics. One of the most important features of microfluidic devices is their ability to generate spatial and temporal perturbations in extracellular environments, and we discuss how this has led to new insights into cellular signalling. Finally, we briefly describe how these tools can be applied to studies beyond single cells.

### Quantifying fluorescent protein levels *in vivo*

For synthetic biologists, the main tools for quantifying gene activity *in vivo* are fluorescent proteins. These proteins can be used to measure gene activities by either placing them behind a promoter of interest or fusing them to a target protein. Since the discovery of GFP in 1962 (REF. 15), a host of fluorescent protein variants<sup>16</sup> have been developed, and their use has become widespread in various applications. A wide range of colours is available<sup>17</sup>, allowing the simultaneous measurement of two or more proteins. For instance, this technique was used by Elowitz *et al.* to measure the relative contributions of intrinsic noise and extrinsic noise in gene expression<sup>18</sup>. In addition, by tagging mRNA-binding proteins with fluorescent proteins, several groups have been able to track both the spatial and the temporal activity of transcripts<sup>19–22</sup>. Several effective tools are available for quantifying fluorescent protein levels in cells; the most common of these are flow cytometry and fluorescence microscopy.

**Flow cytometry.** The most popular method for measuring the activities of fluorescent proteins in living cells has been flow cytometry, which is an easy-to-use, high-throughput method. Using flow cytometry, researchers can quickly analyse hundreds of thousands of cells and generate a snapshot of the distribution of the activity of a gene in a population of cells. The major drawback of this method is that once a cell is measured, it is discarded. Therefore, the dynamics of gene activity in single cells cannot be ascertained. At best, time-lapse flow cytometry can be used to study the fluorescence distribution of a population over time. This technique can be used accurately, especially if the cell population has been synchronized. For instance, Stricker *et al.* used time-lapse flow cytometry to measure the period of a synthetically constructed gene oscillator in a synchronized culture of *Escherichia coli*<sup>23</sup>. However, the synchronization of the culture does not last long because the noise inherent in gene expression<sup>18,24</sup> creates phase diffusion in the oscillators. Although each cell continues to oscillate, the relative timing among the members of the population becomes randomized after only a few oscillations. Thereafter, the dynamics of the population will no longer be measurable from any population average, and it will become necessary to measure time-lapse data from single cells.

**Fluorescence microscopy.** Another widely used technique for quantifying gene activity is fluorescence microscopy. With this method, the fluorescence of individual cells

can be quantified with great accuracy and with high enough resolution to determine the spatial distribution of fluorescence. The major drawback of fluorescence microscopy is that it cannot quantify the fluorescence of thousands of cells simultaneously, which is possible with flow cytometry. Therefore, fluorescence microscopy limits the accuracy of calculations that describe the fluorescence distribution of the population. However, fluorescence microscopy has a major advantage over flow cytometry in that individual cells can be imaged multiple times for long durations, which allows time-lapse fluorescence measurements to be made that are not averaged over the population. When studying the dynamics of gene expression in single cells, this type of data is important.

Time-lapse fluorescence microscopy (TLFM) has become one of the preferred methods among synthetic biologists for studying the dynamics of intracellular signalling and gene networks<sup>25</sup>. The temporal expression data that can be obtained from TLFM are invaluable for the characterization and mathematical modelling of gene networks, especially those networks for which dynamic control is important. Dynamic models of gene regulation often suffer from a lack of knowledge of parameter values, and TLFM helps to put constraints on these models (BOX 1). In addition, recent work has shown that temporal correlations in gene expression can reveal the structure of the underlying regulatory network<sup>26</sup> because autoregulatory motifs can help to determine the range of gene expression noise<sup>27</sup>.

However, there are still major limitations to TLFM. First, phototoxic and photobleaching effects<sup>28</sup> limit the duration of excitation (reducing signal to noise ratios) and the frequency of image capture (reducing temporal resolution). Second, fluorescent proteins take time to mature before they are active and are stable once produced — both of these properties severely limit their dynamic range. These problems can be alleviated with the use of fluorescent proteins that are fast to mature<sup>29</sup> or that are tagged with degradation sequences<sup>30–32</sup>. Finally, TLFM requires cells to remain almost motionless in the focal plane for long durations. The use of commercially available flow chambers can solve this problem, especially for mammalian cells that adhere to surfaces, and flow chambers for yeast cells are also now available<sup>33</sup>.

Microfluidic devices are an increasingly popular, inexpensive and easy-to-use alternative that can be custom-designed to fit the needs of specific experimental protocols. As we describe in the next few sections, microfluidic devices make it possible to trap cells for TLFM and to study the response of those cells to environmental perturbations at the level of a single cell and, increasingly, at the level of organisms and populations.

### The rise of microfluidic devices

Much of the early work involving microfluidics in biology focused on biochemical assays of small concentrations of DNA and proteins<sup>34–38</sup>. Since then, the complexity of microfluidic chips designed for this purpose has grown quickly<sup>39</sup>. For example, devices have

#### Intrinsic noise

Random, stochastic fluctuations in gene expression caused by a small number of reactants interacting in a finite volume.

#### Extrinsic noise

Fluctuations in gene expression that are not caused by intrinsic noise.

#### Time-lapse fluorescence microscopy

The repeated imaging of fluorescent markers using microscopy over a period of time, thus allowing a movie of the dynamics of gene expression or signalling networks to be obtained.

been created that consist of an array of chambers that can be controlled individually using valves and switches and thereby allow biochemical experiments to be performed in parallel<sup>40–42</sup>. The work of Quake and colleagues exemplifies this line of microfluidic research, creating integrated devices that allow the long-term analysis of cells in a microfluidic bioreactor<sup>43</sup>, the extraction of mRNA from single cells and the subsequent synthesis of cDNA by PCR<sup>44</sup>, and the highly parallel measurement of transcription factor–DNA binding affinities<sup>45</sup>.

Some early chips were designed to mimic fluorescence-activated cell sorters<sup>46</sup> or to otherwise manipulate the

movements of cells on a chip<sup>47,48</sup>. However, to examine intracellular signalling and dynamic gene regulation, it is necessary to track individual cells through time. To this end, several groups have designed devices that trap either single cells or small populations of cells for long-term imaging<sup>49–54</sup>. Other groups have concentrated not just on trapping cells, but also on manipulating their environment. For instance, Whitesides and colleagues have created a series of chips that can create spatial gradients in extracellular chemical concentrations<sup>55–57</sup>. Similarly, one can use microfluidic devices to create temporal changes in the growth medium, and this technique has been used in several recent studies<sup>33,58–60</sup>.

### Box 1 | Modelling the dynamics of gene networks

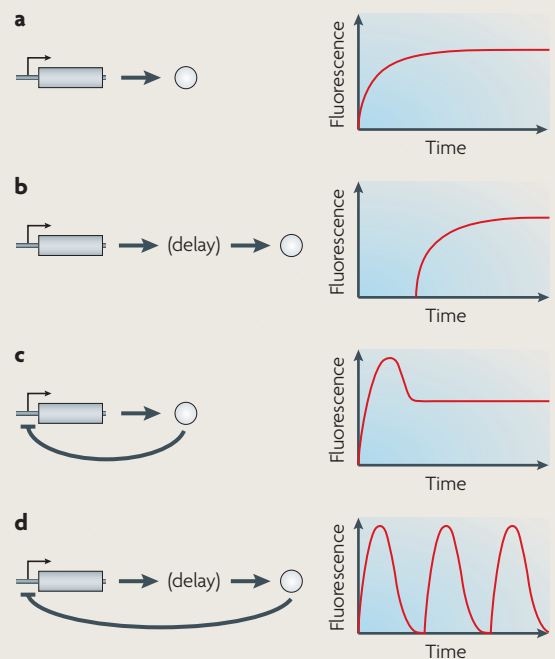
The mathematical modelling of gene regulatory networks began in the mid-1970s with groundbreaking studies such as those by Glass and Kauffman<sup>110</sup> and Savageau<sup>111</sup>. However, our recently acquired ability to create and probe gene networks has revealed that our understanding of the dynamic processes underlying gene regulation is incomplete. Dynamic data are crucial to understanding signalling networks because they constrain the possible parameters and network connections in ways that static (steady-state) data cannot.

For example, consider the four situations depicted in the figure, each of which represents a simple gene network and its resulting dynamics following induction. The four networks are (a) simple constitutive production, (b) constitutive production with delay, (c) negative feedback and (d) negative feedback with delay. If flow cytometry were used to calculate the mean fluorescence of the reporter at the end of each run, this quantity would be the same for each of the four networks shown. This is true even for the fourth example, d, which depicts the dynamics of a delayed negative-feedback oscillator<sup>112</sup>. Owing to intrinsic noise, each individual cell will have a randomized phase relative to the others. Therefore, the average fluorescence over the population of the oscillator will be phase-averaged over the oscillation, resulting in a stationary mean similar to those in examples a–c. If one had access only to long-term stationary data, many types of mathematical models would fit the data<sup>113</sup>; therefore, determining which type of model is the 'correct' model is nearly impossible in this situation.

Researchers have formulated various mathematical techniques for modelling the behaviour of gene networks<sup>114,115</sup>, and in some cases these models have revealed hidden network connections or accurately predicted qualitative behaviours<sup>60,116</sup>. However, many mathematical models do a poor job of predicting the dynamics, such as feedback and feedforward loops, of even simple gene networks that consist of one or two genes.

There are several reasons for this. First, the experimental techniques and quantifiable reporters needed to study the finer details of gene networks have only recently been developed. Second, there is a lack of knowledge of the parameter values, such as binding affinities and degradation rates, that are crucial for creating accurate dynamic models. Finally, there is a lack of specific knowledge about network components, such as network connections and reaction pathways.

The most popular mathematical models are mass action-based systems of ordinary differential equations (ODEs). If the underlying chemical reactions of the network are known, then it is simple to write down the corresponding ODEs. Unfortunately, one rarely knows all of the chemical reactions that take place in a gene network, and the total number of all possible chemical reactions is overwhelming, even for 'simple' one- or two-gene systems. For example, the process of producing one protein involves so many enzymes and sub-steps that the resulting set of ODEs is extremely large. To alleviate this problem, theorists have created reduced models that, it is hoped, approximate the dynamics of the whole system<sup>117,118</sup>. There are known problems with these methods, such as stochasticity<sup>18,24,114,119,120</sup>, delay<sup>112,121–124</sup> and timescale errors<sup>114,125,126</sup>, and it is as yet unknown when these errors are important and when they can be ignored. Despite this, dynamic, ODE-based modelling has been used successfully to describe phenomena such as genetic toggle switches<sup>127</sup>, synthetic oscillations<sup>128</sup>, osmo-adaptation signalling<sup>58</sup> and metabolic responses to fluctuating environments<sup>60</sup>.



**Bacterial persistence**

Similar to antibiotic resistance, bacterial persistence is the phenomenon by which a fraction of a genetically homogeneous bacterial colony will survive antibiotic treatment but retain antibiotic sensitivity following regrowth.

**Polydimethylsiloxane**

An optically clear organic polymer that is commonly used for soft lithography.

**Stochastic**

Probabilistic; governed by chance.

**Microfluidic devices for single-cell TLFM**

The best way to examine the dynamics of individual cells is to capture a single cell, hold it in place for a long period of time and take measurements. For many types of cell this can be a problem, especially as they grow, divide and move with fluid flows. Cells can be immobilized in various ways, such as by taking advantage of surface adherence properties<sup>61</sup>, chemically attaching them to the chamber<sup>58</sup> or even impaling them with synthetic nanostructures<sup>62</sup>. However, for many studies, these solutions are not viable. Instead, some groups are creating microfluidic chips that put physical constraints on the movement of cells.

In one of the first studies that used microfluidics to constrain cells for long-term study, Balaban *et al.* forced *E. coli* cells to grow in linear chains derived from a single cell to investigate the switch-like behaviour of bacterial persistence<sup>63,64</sup>. To do this, they created a flow chamber-like device in which the cells grew on a layer of polydimethylsiloxane (PDMS) that had been moulded to form grooves, each with a width similar to that of a single *E. coli* cell. A permeable membrane and PDMS flow chamber were placed on top of this layer to supply media and antibiotics (FIG. 1). The authors showed that bacterial persistence is linked to pre-existing gene expression heterogeneity in the population, and from the data obtained they were able to create a mathematical model that accurately described the phenomenon. The method used by Balaban *et al.* worked well for investigating bacterial persistence. The linear chains created by the grooves made it easy to discern lineages among the cells, and the height constraints limited the cells to a monolayer for easy focus. However, the complex, multilayer design makes the device difficult to assemble.

In more recent designs, the number of layers has been reduced by the bonding of a single piece of moulded PDMS directly onto glass coverslips. Several groups have created 'microchemostats'<sup>50,51</sup> with this simplified design to mimic the function of microbioreactors<sup>65,66</sup>. For example, Cookson *et al.* used the Tesla microchemostat<sup>51,60</sup> to examine the expression of fluorescent protein in single

cells of *Saccharomyces cerevisiae* over many generations (FIG. 2). These types of devices have proved useful, but are not without their limitations. As the colonies grow, fluid lines going into or out of the chip can clog with cells, and the efficiency at which the devices constrain the population size decreases. Furthermore, there is no guarantee that an individual cell will stay in the chamber. However, long-term acquisition of single-cell trajectories is possible, and the total duration depends on the organism and chip design. Various versions of the Tesla microchemostat can support log-phase growth of *E. coli* for 4–10 hours and *S. cerevisiae* for 24–48 hours, depending on the conditions.

Other designs have refined single-cell tracking even further. Ryley and Pereira-Smith recently created a microfluidic chip designed to individually trap *S. cerevisiae* cells in small compartments, or 'jails'<sup>52</sup> (FIG. 3a,b). Aliquots of cell suspensions are placed on top of the arrays, and the cells are allowed to settle into the jails. As the cells grow and divide, the geometry of the jail forces the bud outside the 'bars'. Once the bud detaches, it is washed away by the flow of the surrounding fluid, leaving the mother cell trapped inside the jail. Similarly, Di Carlo *et al.* have also trapped single cells for long-term data acquisition. They used an inverted catching design (FIG. 3c–e) to trap individual cells and examine enzyme kinetics in mammalian HeLa, 293T and Jurkat cells<sup>54</sup>. Like Ryley and Pereira-Smith's chips, this design was highly paralleled so that many individual cells could be trapped simultaneously.

Other groups have reported chip designs that can trap either single cells or small populations of cells<sup>67,68</sup>, and these have been used in numerous observational studies, including analysis of the pheromone response of *S. cerevisiae*<sup>69</sup>, the long-term growth of mammalian cells<sup>49</sup>, drug screening at the single-cell level<sup>70</sup>, intercellular Ca<sup>2+</sup> flux measurements<sup>71</sup>, the dynamics of the nuclear factor- $\kappa$ B response in mammalian cells<sup>72</sup>, the adhesion properties of cells in response to shear stress<sup>73</sup>, stochastic protein expression<sup>53</sup>, hepatic inflammation<sup>74</sup> and the biomechanical ordering of growing bacterial populations<sup>75,76</sup>.

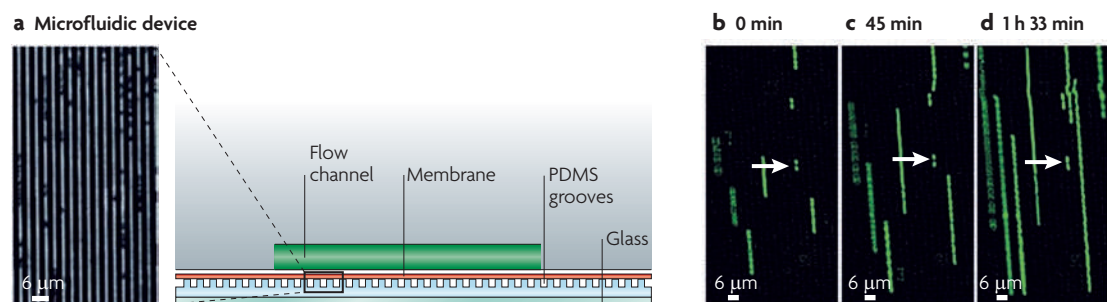


**Figure 1 | A microfluidic device for monitoring *Escherichia coli*.** **a** | A schematic of the device used by Balaban *et al.* in their study of bacterial persistence<sup>63</sup>. The device consists of four layers. On top of the glass base resides a grooved layer of polydimethylsiloxane (PDMS) for growing linear chains of bacteria. A permeable membrane rests on top of the grooved PDMS to constrain the cells to the focal plane and allow media to pass into the growth chamber. Above the membrane lies another layer of PDMS that houses the media flow channel. **b–d** | Representative time-lapse images of *E. coli* expressing yellow fluorescent protein taken approximately 45 minutes apart from each other. Figure is reproduced, with permission, from REF. 63 © (2004) American Association for the Advancement of Science.



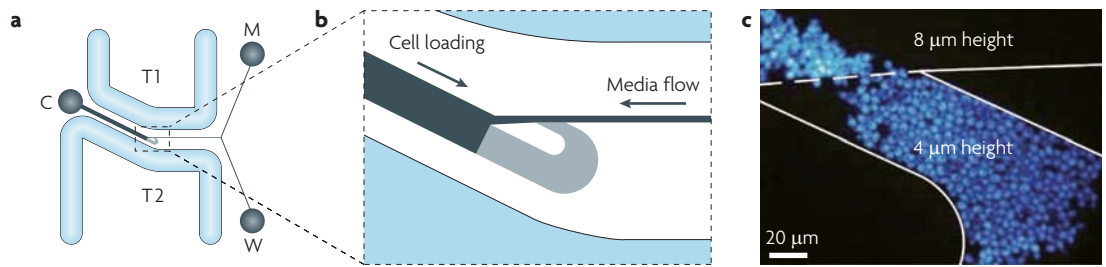


**Figure 2 | The Tesla microchemostat.** **a** | Cells are loaded through reservoirs leading into port C and trapped in the imaging region (which is enlarged in part **b**). Once enough cells are trapped, the flow is reversed by increasing the pressure in the media inlet, port M. Excess media is routed through port W (waste). Heated water is passed through two channels (labelled T1 and T2) on either side of the imaging chamber to control the temperature on the chip. **b** | A close-up diagram of the imaging region. Once the flow has reversed, the trapping region (grey) is isolated from the flow and only receives nutrients through diffusion. **c** | A typical fluorescence image of *Saccharomyces cerevisiae* expressing GFP. The height of the imaging chamber is 4  $\mu\text{m}$ , which forces the cells to grow in a monolayer and creates a uniform focal plane. Outside the chamber, the channels are twice as tall, which allows cells to be easily washed away by the flow. Figure is reproduced, with permission, from REF. 51 © (2005) Macmillan Publishers Ltd. All rights reserved.

These pioneering studies demonstrated the efficacy of using lab-on-a-chip approaches for the long-term study of gene expression. But these devices are merely an alternative to other methods for examining cells, such as flow chambers and even simple agar pads. The real benefit of using microfluidic devices comes when one takes advantage of the ease with which microscale fluid flows can be manipulated both temporally and spatially to control environmental conditions. Such manipulation is now possible with the next generation of microfluidic chips.

#### Controlling the environment on microfluidic chips

To survive and thrive, cells must be able to react and adapt to changes in environmental conditions. Gene regulatory networks and cellular signalling pathways often determine cellular responses to environmental perturbations, and experimental techniques aimed at probing these signalling mechanisms require the ability to precisely control extracellular conditions.

**Generating spatial gradients.** Researchers are now using microfluidic devices to generate spatial gradients in chemical concentrations. This line of research is broadly applicable because many cellular signalling pathways can detect chemical gradients and respond accordingly. For instance, bacterial chemotaxis is mediated by sensing gradients in nutrients, which allows cells to move towards regions more suitable for growth. Similarly, the pheromone response of *S. cerevisiae* enables it to detect gradients of  $\alpha$ - or a-factor, thus allowing haploid cells to mate with cells of the opposite mating type.

One commonly used method for generating spatial gradients with microfluidic devices was developed by Jeon *et al.*<sup>55</sup> and later expanded on by Dertinger *et al.*<sup>56</sup> (both from the Whitesides laboratory). The technique involves the repeated combination and mixing of separate inputs through a network of channels (FIG. 4). With devices such as these, Jeon *et al.* studied the chemotactic behaviour of human neutrophils in various types of chemical gradients<sup>57</sup>. They placed cells on one side of a chamber containing a concentration gradient of

chemoattractant with a maximum concentration in the middle of the chamber. As expected, cells sense the gradient and move towards the maximum. However, the behaviour of the cells also depends on the spatial gradient on the other side of the maximum. If the concentration of chemoattractant on the other side of the maximum gradually falls back to zero, cells move slightly beyond the maximum before turning back. However, when the researchers configured the device to create a precipitous fall on the other side of the maximum (like a sawtooth wave), the cells reach the maximum and abruptly halt. These findings suggested that the gradient-sensing mechanism in neutrophils is more adaptive than previously thought — it temporarily ignores slight changes in the gradient but immediately reacts to large ones.

In another study, Hao *et al.* used a microfluidic chip that could create chemical gradients to study the response of *S. cerevisiae* to differing concentrations of pheromone<sup>77</sup>. As yeast cells are exposed to pheromone they undergo morphological changes that lead to elongated growth or growth arrest, depending on the concentration of pheromone. Interestingly, the same kinase cascade is responsible for both of these phenotypes. Two similar protein kinases, *Fus3* and *Kss1*, mediate these outcomes, but it was unclear how they discriminate between conditions. Using their gradient device in combination with mathematical modelling, Hao and colleagues showed that the scaffold protein *Ste5*, which brings together various proteins in the mitogen-activated protein kinase (MAPK) cascade, dynamically regulates the activity of *Fus3* but not *Kss1*. Whereas *Kss1* exhibits a fast, graded response to doses of pheromone, *Ste5* slows the response of *Fus3* and confers a switch-like, ultrasensitive dose-response profile upon it.

Other designs for creating spatial gradients in microfluidic devices have also been developed<sup>78–83</sup>; these have been used to examine phenomena such as bacterial<sup>84,85</sup> and T cell chemotaxis<sup>86</sup>, neural stem cell differentiation<sup>87</sup> and the yeast pheromone response<sup>88</sup>. Some groups have also combined gradient generation with dynamic control to create devices capable of changing chemical gradients over time<sup>89,90</sup>.

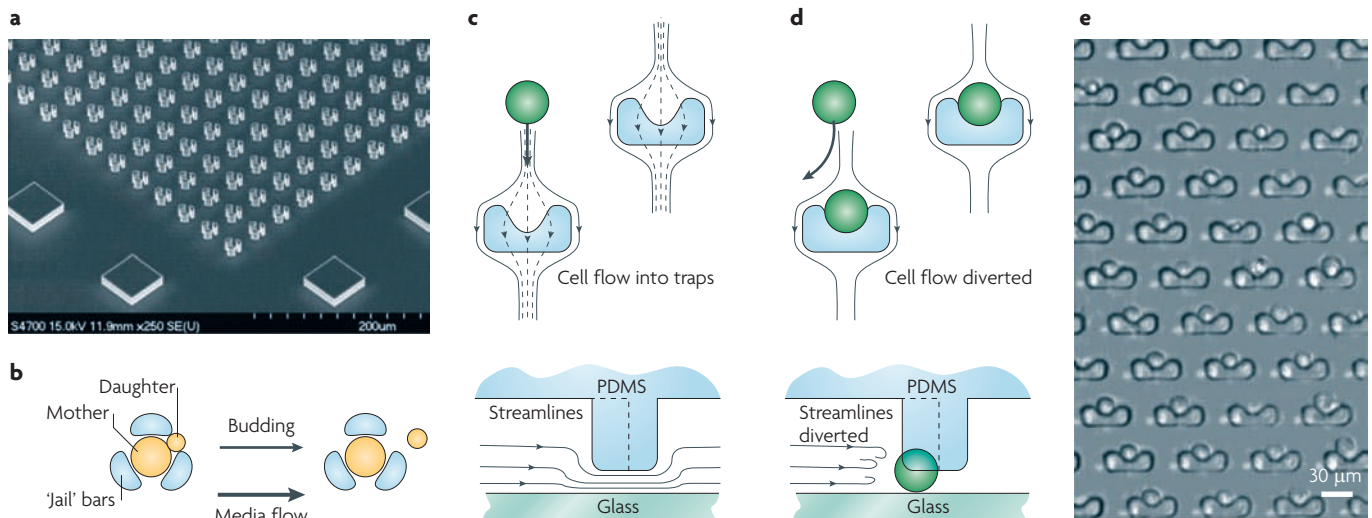


**Figure 3 | Microfluidic trapping devices designed for the long-term acquisition of single-cell data.** **a** | The device designed by Ryley *et al.* has an array of single-cell 'jails' that can trap yeast cells<sup>52</sup>. **b** | As cells grow and divide in the jail, the geometry forces the daughter cell outside the jail, where it is flushed away by media flow. Di Carlo *et al.* designed a similar trap for mammalian cells<sup>54</sup>. **c** | Cells (green circles) are loaded through the array, in which they are trapped by low-hanging areas of polydimethylsiloxane (PDMS; light blue). **d** | Fluid flow helps to keep the cell trapped against the PDMS, and other cells are diverted around the PDMS. **e** | A microscope image of an array of these traps, showing individual cells. Part **a** is reproduced and part **b** is modified, with permission, from REF. 52 © (2006) Wiley. Parts **c** and **d** are modified and part **e** is reproduced, with permission, from REF. 54 © (2006) American Chemical Society.

**Cellular responses to temporally varying environments.** Microfluidic devices also now exist that can temporally control chemical concentrations. Early work in this field has focused on reverse engineering or characterizing cellular pathways<sup>33,58–60,91</sup>. For instance, Mettetal *et al.* used a computer-controlled valve system to create a square wave of NaCl pulses that was injected into a flow chamber to measure the response of the osmo-adaptation pathway in *S. cerevisiae*<sup>58</sup>. This pathway, which responds to osmolarity changes through the high-osmolarity glycerol MAPK cascade, is of particular interest because it contains two negative-feedback loops that act on different timescales. One of these loops, which is governed by the association and dissociation of ligands and receptors of the kinase cascade, is extremely fast, whereas the other, which is mediated by transcriptional regulation and protein synthesis, is much slower. By subjecting cells to periodic stimuli of various frequencies and comparing the results with mathematical models, Mettetal *et al.* found that these two feedback loops have distinct biological functions. As expected, the fast feedback loop dominates the main response of the pathway. However, as a result of their mathematical modelling, the authors found that the slow feedback loop allows cells to respond even faster to future stimuli, especially after large osmotic shocks.

In a similar study, Bennett *et al.* combined a microfluidic chip with a variable pressurization system that could create user-defined temporal waveforms to examine the transcriptional response of the glucose–galactose switch in *S. cerevisiae*<sup>60</sup>. To do this, they programmed a device, which they termed the 'dial-a-wave' (FIG. 5), to sinusoidally vary glucose concentrations over a galactose background. They then measured the expression of

a fluorescent reporter fused to *GALI*, a key player in the galactose utilization network. Because the galactose utilization network is so well characterized, the authors could create a detailed computational model incorporating the known reactions and compare it with their experimental results. Interestingly, they found that although static data obtained from flow cytometry matched their model well, the dynamic data obtained from the TLFM experiments did not. To reconcile the model with their data, Bennett *et al.* proposed a previously undiscovered form of post-transcriptional regulation in the galactose–glucose switch. They surmised, and verified through additional experiments, that the transcripts produced from *GALI* (which encodes a galactokinase that initiates galactose catabolism) and *GAL3* (which encodes a regulatory protein that confers a positive-feedback response to the galactose network) are less stable in glucose-rich environments. Therefore, the coupling of TLFM and mathematical modelling led directly to the discovery of a new regulatory mechanism in this well-studied network.

The two studies by Mettetal *et al.* and Bennett *et al.* show the benefit of using dynamic perturbations, TLFM and mathematical modelling to study intracellular signalling pathways (FIG. 6). In both studies, they were able to discover new phenomena as a consequence of their mathematical modelling. Furthermore, they were able to 'train' their models based on the dynamic data that were obtained through microfluidics, thus revealing insights that would otherwise have been obscured. It is also interesting to note that the kinds of mathematical models the two groups used were different. For their study, Mettetal *et al.* used principles of linear systems theory that are common in engineering. This type of model requires

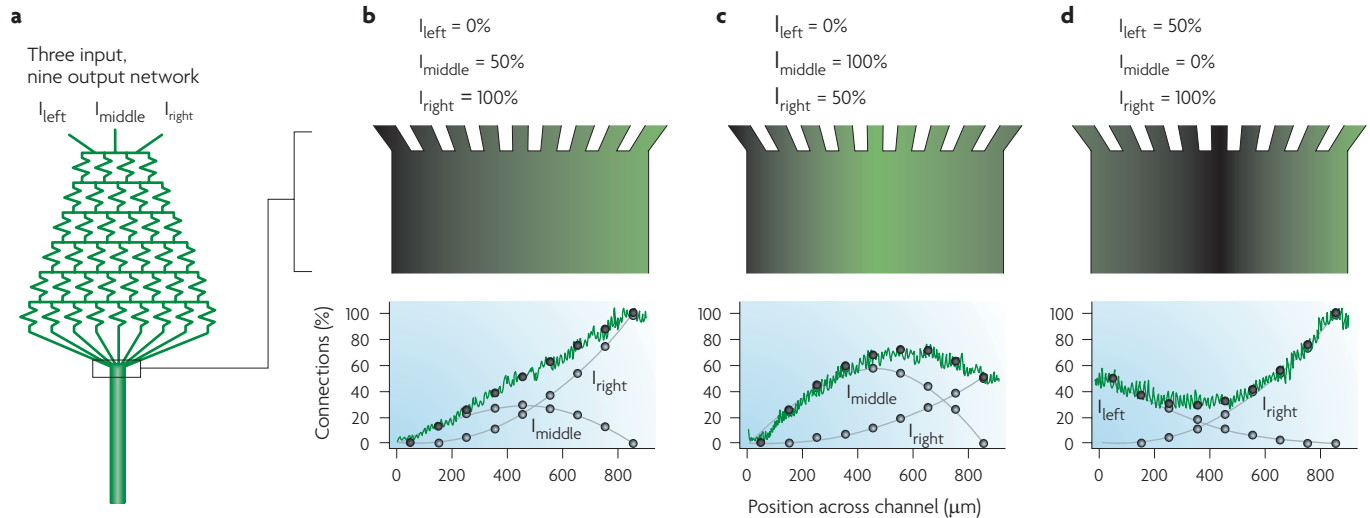


Figure 4 | **A microfluidic device designed for generating concentration gradients.** **a** | Schematic of the device. There are three inlet ports (labelled  $I_{left}$ ,  $I_{middle}$  and  $I_{right}$ ), which feed down through a diffusion array to the imaging chamber. **b–d** | Depending on the make-up of the three inlet ports, various spatial gradients can be achieved. Figure is reproduced, with permission, from REF. 56 © (2001) American Chemical Society.

little knowledge of the underlying biological mechanisms but still provides insights into the dynamics. By contrast, Bennett *et al.* created a model that tried to incorporate as many known biochemical reactions as was feasible. These types of models may be more complete, but they suffer from a lack of knowledge of the parameter values. Even so, the model created by Bennett *et al.* accurately simulated the data and made testable predictions that they subsequently verified experimentally.

There are also several alternative ways of achieving dynamic control of chemical concentrations in chips<sup>92–97</sup>. Some laboratories have even created parallel designs that can deliver temporal chemical stimulation to multiple imaging chambers simultaneously for high-throughput analysis<sup>98</sup>. Taylor *et al.* recently used this type of technique to examine the pheromone response and MAPK signalling in *S. cerevisiae*<sup>99</sup>. Furthermore, microfluidic devices that can generate time-dependent signals have also been developed for studying mammalian cells. For instance, Higgins *et al.* used a microfluidic device to control the oxygen content of a streaming channel of blood cells to study the vaso-occlusion caused by sickle cell disease<sup>100</sup>. They found that the polymerization and melting of sickle cell haemoglobin, which depend on the oxygen concentration, are enough to recreate occlusion and rescue, respectively. Polinkovsky *et al.* later arrived at a similar solution; by temporally controlling the mixing of two gases before their delivery to cell-growth and imaging chambers, they were able to study the oxygen-dependent growth rate of *E. coli*<sup>101</sup>.

**Limitations**

There are still some major limitations to using microfluidic devices for the creation of spatial and temporal environmental perturbations. The flow of fluid in the chips must be precisely controlled to accurately generate the desired gradients or changes; however, as the cells grow and divide, the fluidic resistances inside

the channels change, which causes diversions or even blockages of the fluid flows. Because of this, it can be difficult to maintain precise gradients and waveforms for long periods of time.

The creation of better cell traps should help to alleviate this problem. Newer devices control the population size and wash away unwanted cells more efficiently than the first generation of lab-on-a-chip approaches. Furthermore, even with the problem of maintaining fluid flow, microfluidic devices are still the best option for examining cellular responses to environmental perturbations — especially when single-cell resolution is necessary.

**Beyond single cells**

In addition to examining single-cell dynamics, which we have focused on in this Review, researchers are using microfluidic devices to examine higher-level phenomena<sup>50,75,76,102–105</sup>. Often, cells exhibit behaviours as a group that do not manifest at the single-cell level. For instance, many types of bacteria can detect fluctuations in cell density through quorum-sensing signalling molecules<sup>106</sup>. Balagaddé *et al.* used a microfluidic device to study the growth dynamics of a synthetically altered strain of *E. coli* that transcribes a cell death protein (LacZa–CcdB) at high cell densities<sup>43</sup>. They found that when the synthetic circuit is turned off, cell densities initially increase exponentially before eventually saturating, as expected. However, when the circuit is turned on, the cell densities oscillate over time. This occurs because the initial concentration of the intercellular signalling molecule acyl-homoserine lactone (AHL) is too low to induce expression of the cell death protein. Then, as cell densities rise, so does the concentration of AHL, subsequently initiating transcription of LacZa–CcdB. As cells die, the concentration of AHL declines, resulting in lowered transcription of LacZa–CcdB, which allows cellular growth to begin anew.

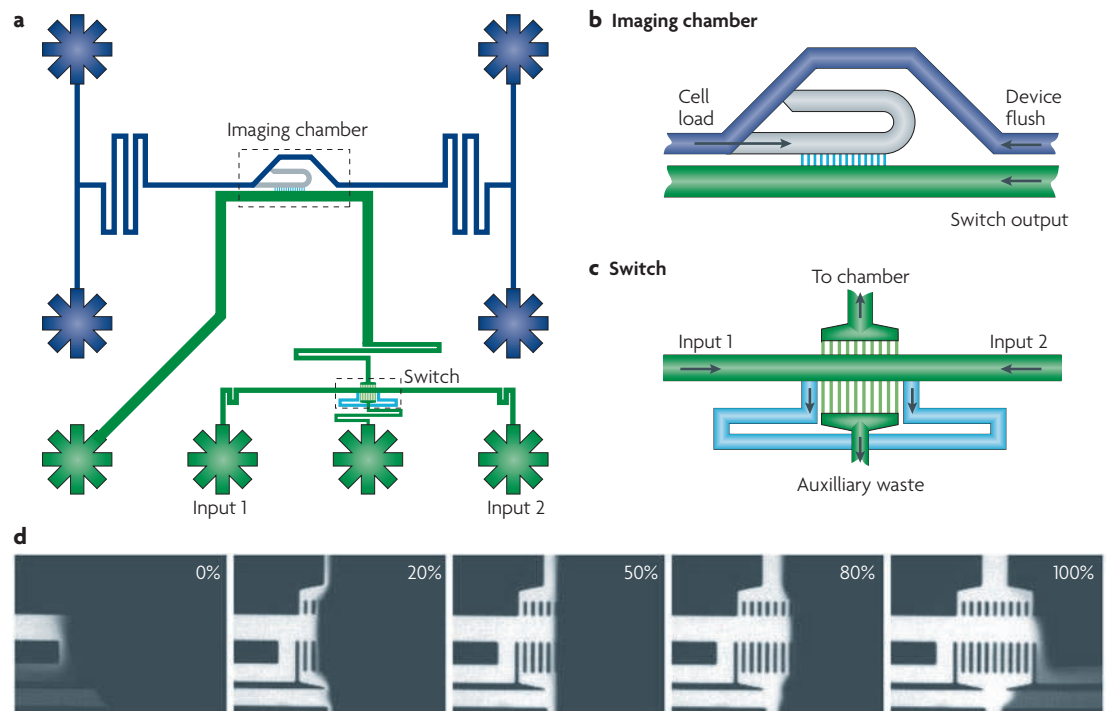


**Figure 5 | The microfluidic ‘dial-a-wave’ device.** **a** | The overall design of the dial-a-wave device is similar to that of the Tesla microchemostat<sup>51</sup>. Cell input channels (dark blue) feed into an imaging chamber (grey), in which cells are trapped for long periods of time. The growth medium for the imaging chamber is supplied by a switching channel system (switch; green channels) that can provide programmable, time-dependent concentration waves. **b** | As the growth medium (in the green channel) flows near the imaging chamber, small perfusion channels (light blue) allow the medium to diffuse into the cell culture. **c** | The switch region determines the make-up of the medium supplied to the imaging chamber. Two inputs, labelled input 1 and input 2 in **a** and **c**, feed into the switch region. Owing to the small flow rates and the geometry of the channels, the interface between the two inputs is laminar, which allows for precise control over the mixing ratio. **d** | By differentially pressurizing the two input reservoirs, the laminar interface can be moved from one side of the switching region to the other. In this way, the relative concentrations of the two media can be programmed to any desired waveform. Figure is modified, with permission, from *Nature* REF. 60 © (2008) Macmillan Publishers Ltd. All rights reserved.

Lucchetta *et al.* used a microfluidic device to study perturbations to the patterning network of *Drosophila melanogaster* embryos<sup>107</sup>. During *D. melanogaster* embryonic development, the *even-skipped* gene is expressed in seven evenly spaced stripes of high and low expression levels along the anteroposterior axis of the embryo. The device creates two separate laminar aqueous flows of different temperatures, thus subjecting *D. melanogaster* embryos to thermal perturbations along the anteroposterior axis. In this manner, the authors affected the relative growth rates of the two halves of the embryo, because warmer sections develop faster. Contrary to expectation, the patterning network was found to be robust to perturbation by the heat treatment. However, differential growth rates of the two halves of the embryo led to abnormal temporal development of the stripes. Under normal conditions the stripes resolve in a specific order, but when a temperature gradient is introduced this ordering is changed.

Another study, by Keymer *et al.*, used microfluidic devices to study the population dynamics of competing strains of *E. coli*<sup>105</sup>. The authors simultaneously grew two strains of *E. coli* in coupled ‘microhabitat patches’<sup>104</sup>

and observed their growth patterns over multiple days. One of the strains carried a *gasp* (growth advantage in stationary phase) mutation that should have allowed the mutant strain to outcompete the wild type. Interestingly, Keymer *et al.* found that when the two strains are allowed to compete, the overall fitness of both strains is greater than when they are grown in isolation — providing that the medium is nutrient rich. Although they have no explanation for why this effect occurs, they were able to demonstrate that the phenomenon has strong spatiotemporal aspects.

These studies illustrate the myriad possibilities of using microfluidic devices for studying gene regulation beyond single cells. They also reveal a particularly intriguing problem for mathematical biologists. How does one go about modelling phenomena that originate at small scales (for example, as genes and proteins) yet manifest at large scales (for example, as developmental processes and interspecies fitness)? There is still no good answer to this question. Future studies will greatly benefit from microfluidic devices, because they give researchers more environmental control over small cellular populations than any other method.



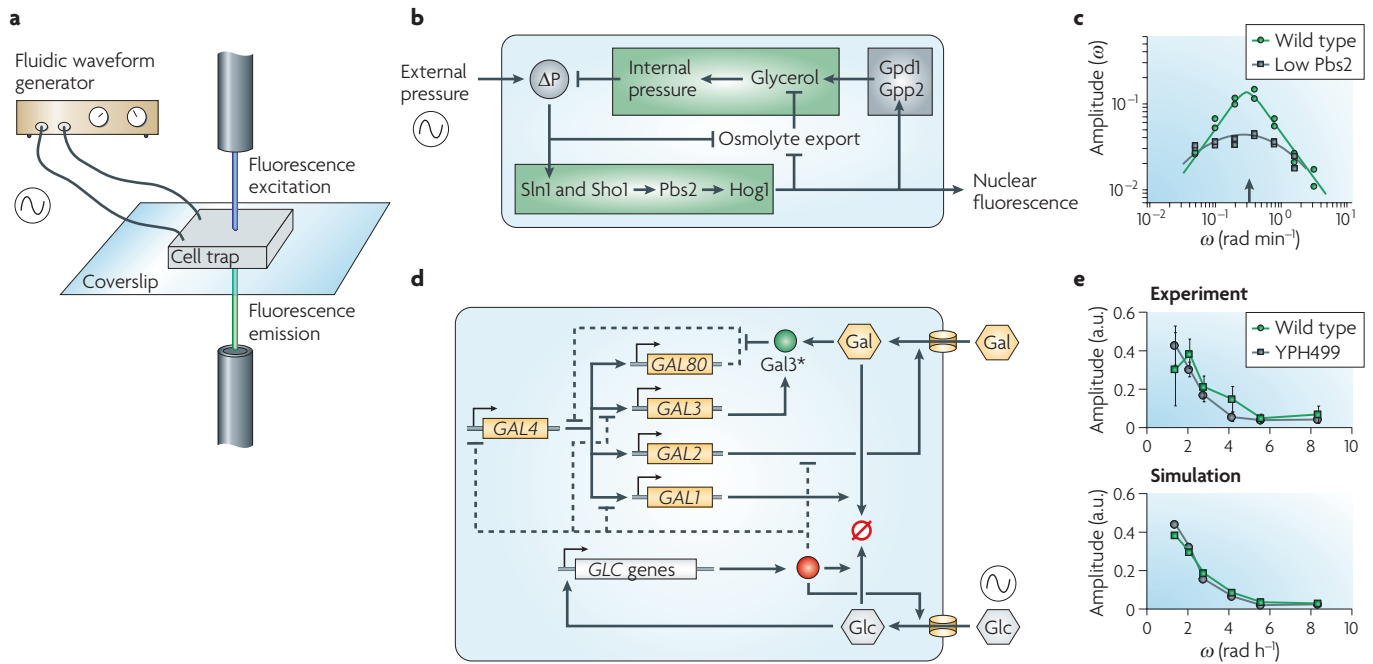


Figure 6 | **Temporal driving with microfluidic chips to test mathematical models.** **a** | The concentrations of key components of the growth media are controlled, or ‘driven’, by a fluidic waveform generator. In the chip, cells are continually measured with fluorescence microscopy as they react to the changing media conditions. Setups similar to this have been used by several groups to explore signalling pathways in *Saccharomyces cerevisiae*. **b** | Mettetal *et al.*<sup>58</sup> drove the high-osmolarity glycerol (HOG) pathway in yeast and discovered key signalling characteristics for wild-type and network-deficient strains. **c** | The dynamic data obtained were used to validate and refine the mathematical model. The graph compares wild-type *S. cerevisiae* with a strain expressing a reduced amount of Pbs2 (polymyxin b sensitivity 2). **d** | Bennett *et al.*<sup>60</sup> drove the galactose utilization network in yeast with periodic carbon source changes and found new network connections. **e** | The dynamic data obtained from the experiment were used to validate and refine the mathematical simulation. The data show how the network created a low-pass filter. YPH499 is an *S. cerevisiae* strain that exhibits reduced galactose sensitivity in static environments. a.u., arbitrary units; Gal, galactose; Gal3\*, Gal3 bound to galactose; Glc, glucose; Gpd1, glycerol-3-phosphate dehydrogenase 1; Gpp2, (DL)-glycerol-3-phosphatase 2; P, pressure. Parts **b** and **c** are reproduced, with permission, from REF. 58 © (2008) American Association for the Advancement of Science. Parts **c–e** are reproduced, with permission, from *Nature* REF. 60 © (2008) Macmillan Publishers Ltd. All rights reserved.

**Conclusion**

Microfluidic devices are now at the forefront of research into the dynamics of gene regulation. They, and TLFM techniques in general, are essential tools that allow us to better understand the dynamic ways in which genes determine cellular responses to internal and external stimuli. Through the concerted interplay of experiments and mathematical modelling, general design principles will emerge that will reveal the mechanisms behind native networks and govern the future design of synthetic circuits.

It should be stressed that our understanding of gene regulation is continually evolving, and we are finding that even basic processes can behave in ways that were unexpected several years ago. For instance, Cai *et al.* found that the yeast transcription factor *Crz1* encodes its signal not by nuclear concentration but by frequency-modulated bursts into and out of the nucleus<sup>108</sup>. This is different from past models of transcription factor activity, in which it was not the frequency but the amplitude (that is, the concentration) of the signal that determined transcriptional activity.

Transcriptional regulation has been at the heart of many theoretical studies of gene networks, and we are now finding that the mechanisms by which transcription factors modulate gene activity are more dynamic than once thought.

To further complicate the situation, there is a wide range of techniques for mathematically modelling gene network dynamics<sup>109</sup>, as illustrated by the discussion of the studies from Mettetal *et al.*<sup>58</sup> and Bennett *et al.*<sup>60</sup> above. Which, if either, of these two types of models is the ‘correct’ method? Systems-level models that obscure molecular-level reactions but reveal large-scale phenomena, or detailed models that strive for biological accuracy at the expense of analytic tractability? The answer to this is still unclear and is likely to depend on the types of questions being asked of the model. Detailed models, such as that formulated by Bennett *et al.*, delve into the particulars of biochemical pathways in an attempt to elucidate the fundamental mechanisms underlying regulation. By contrast, systems-level models, such as that used by Mettetal *et al.*, are an attempt to examine the dynamics of signalling modules as a whole.

At some level, both types of models are probably correct. Therefore, instead of debating the correctness of one method or the other, a better question to ask might be: at what level of organization, if any, can one ignore

individual molecular interactions and begin to model gene networks in terms of signalling modules? This is just the type of question that microfluidic devices will help us to answer.

1. Koide, T., Pang, W. L. & Baliga, N. S. The role of predictive modelling in rationally re-engineering biological systems. *Nature Rev. Microbiol.* **7**, 297–305 (2009).
2. Reder, C. Metabolic control theory: a structural approach. *J. Theor. Biol.* **135**, 175–201 (1988).
3. Edwards, J. S., Covert, M. & Palsson, B. Metabolic modelling of microbes: the flux-balance approach. *Environ. Microbiol.* **4**, 133–140 (2002).
4. Cline, M. S. *et al.* Integration of biological networks and gene expression data using Cytoscape. *Nature Protoc.* **2**, 2366–2382 (2007).
5. Hasty, J., McMillen, D. & Collins, J. J. Engineered gene circuits. *Nature* **420**, 224–230 (2002).
6. McDonald, J. C. *et al.* Fabrication of microfluidic systems in poly(dimethylsiloxane). *Electrophoresis* **21**, 27–40 (2000).
7. Whitesides, G. M., Ostuni, E., Takayama, S., Jiang, X. Y. & Ingber, D. E. Soft lithography in biology and biochemistry. *Ann. Rev. Biomed. Eng.* **3**, 335–373 (2001).
8. Ng, J. M., Gitlin, I., Stroock, A. D. & Whitesides, G. M. Components for integrated poly(dimethylsiloxane) microfluidic systems. *Electrophoresis* **23**, 3461–3473 (2002).
9. **References 6–8 are good reviews covering the design and manufacture of microfluidic devices.**
10. Sia, S. K. & Whitesides, G. M. Microfluidic devices fabricated in poly(dimethylsiloxane) for biological studies. *Electrophoresis* **24**, 3563–3576 (2003).
11. Lidstrom, M. E. & Meldrum, D. R. Life-on-a-chip. *Nature Rev. Microbiol.* **1**, 158–164 (2003).
12. Weibel, D. B., Diluzio, W. R. & Whitesides, G. M. Microfabrication meets microbiology. *Nature Rev. Microbiol.* **5**, 209–218 (2007).
13. Chao, T. C. & Ros, A. Microfluidic single-cell analysis of intracellular compounds. *J. R. Soc. Interface* **5** (Suppl. 2), S139–S150 (2008).
14. Kim, S. M., Lee, S. H. & Suh, K. Y. Cell research with physically modified microfluidic channels: a review. *Lab Chip* **8**, 1015–1023 (2008).
15. Wang, C. J. & Levchenko, A. Microfluidics technology for systems biology research. *Methods Mol. Biol.* **500**, 203–219 (2009).
16. Shimomura, O., Johnson, F. H. & Saiga, Y. Extraction, purification and properties of aequorin, a bioluminescent protein from the luminous hydromedusa, *Aequorea*. *J. Cell Comp. Physiol.* **59**, 223–239 (1962).
17. Zhang, J., Campbell, R. E., Ting, A. Y. & Tsien, R. Y. Creating new fluorescent probes for cell biology. *Nature Rev. Mol. Cell Biol.* **3**, 906–918 (2002).
18. Shaner, N. C., Steinbach, P. A. & Tsien, R. Y. A guide to choosing fluorescent proteins. *Nature Methods* **2**, 905–909 (2005).
19. **References 15–17 detail the properties of various fluorescent proteins that are commonly used in synthetic biology.**
20. Elowitz, M. B., Levine, A. J., Siggia, E. D. & Swain, P. S. Stochastic gene expression in a single cell. *Science* **297**, 1183–1186 (2002).
21. Golding, I., Paulsson, J., Zawilski, S. M. & Cox, E. C. Real-time kinetics of gene activity in individual bacteria. *Cell* **123**, 1025–1036 (2005).
22. Valencia-Burton, M., McCullough, R. M., Cantor, C. R. & Broude, N. E. RNA visualization in live bacterial cells using fluorescent protein complementation. *Nature Methods* **4**, 421–427 (2007).
23. Tyagi, S. Splitting or stacking fluorescent proteins to visualize mRNA in living cells. *Nature Methods* **4**, 391–392 (2007).
24. Haim, L., Zipor, G., Aronov, S. & Gerst, J. E. A genomic integration method to visualize localization of endogenous mRNAs in living yeast. *Nature Methods* **4**, 409–412 (2007).
25. Stricker, J. *et al.* A fast, robust and tunable synthetic gene oscillator. *Nature* **456**, 516–519 (2008).
26. **This study illustrates the maturity of synthetic biology; it reports the creation of a robust and tunable synthetic gene oscillator in *E. coli*.**
27. Swain, P. S., Elowitz, M. B. & Siggia, E. D. Intrinsic and extrinsic contributions to stochasticity in gene expression. *Proc. Natl Acad. Sci. USA* **99**, 12795–12800 (2002).
28. Locke, J. C. & Elowitz, M. B. Using movies to analyse gene circuit dynamics in single cells. *Nature Rev. Microbiol.* **7**, 383–392 (2009).
29. Austin, D. W. *et al.* Gene network shaping of inherent noise spectra. *Nature* **439**, 608–611 (2006).
30. Simpson, M. L., Cox, C. D. & Saylor, G. S. Frequency domain analysis of noise in autoregulated gene circuits. *Proc. Natl Acad. Sci. USA* **100**, 4551–4556 (2003).
31. Cubitt, A. B. *et al.* Understanding, improving and using green fluorescent proteins. *Trends Biochem. Sci.* **20**, 448–455 (1995).
32. Nagai, T. *et al.* A variant of yellow fluorescent protein with fast and efficient maturation for cell-biological applications. *Nature Biotech.* **20**, 87–90 (2002).
33. Rogers, S., Wells, R. & Rechsteiner, M. Amino acid sequences common to rapidly degraded proteins: the PEST hypothesis. *Science* **234**, 364–368 (1986).
34. Andersen, J. B. *et al.* New unstable variants of green fluorescent protein for studies of transient gene expression in bacteria. *Appl. Environ. Microbiol.* **64**, 2240–2246 (1998).
35. Grilly, C., Stricker, J., Pang, W. L., Bennett, M. R. & Hasty, J. A synthetic gene network for tuning protein degradation in *Saccharomyces cerevisiae*. *Mol. Syst. Biol.* **3**, 127 (2007).
36. Charvin, G., Cross, F. R. & Siggia, E. D. A microfluidic device for temporally controlled gene expression and long-term fluorescent imaging in unperturbed dividing yeast cells. *PLoS ONE* **3**, e1468 (2008).
37. Khandurina, J. *et al.* Integrated system for rapid PCR-based DNA analysis in microfluidic devices. *Anal. Chem.* **72**, 2995–3000 (2000).
38. Sanders, G. H. W. & Manz, A. Chip-based microsystems for genomic and proteomic analysis. *Trends Analyt. Chem.* **19**, 364–378 (2000).
39. Lagally, E. T., Medintz, I. & Mathies, R. A. Single-molecule DNA amplification and analysis in an integrated microfluidic device. *Anal. Chem.* **73**, 565–570 (2001).
40. Ramsey, J. D., Jacobson, S. C., Culbertson, C. T. & Ramsey, J. M. High-efficiency, two-dimensional separations of protein digests on microfluidic devices. *Anal. Chem.* **75**, 3758–3764 (2003).
41. McClain, M. A. *et al.* Microfluidic devices for the high-throughput chemical analysis of cells. *Anal. Chem.* **75**, 5646–5655 (2003).
42. Hong, J. W. & Quake, S. R. Integrated nanoliter systems. *Nature Biotechnol.* **21**, 1179–1183 (2003).
43. **This review discusses the use of microfluidic devices for high-throughput biochemical assays.**
44. Anderson, J. R. *et al.* Fabrication of topologically complex three-dimensional microfluidic systems in PDMS by rapid prototyping. *Anal. Chem.* **72**, 3158–3164 (2000).
45. Chiu, D. T., Pezzoli, E., Wu, H., Stroock, A. D. & Whitesides, G. M. Using three-dimensional microfluidic networks for solving computationally hard problems. *Proc. Natl Acad. Sci. USA* **98**, 2961–2966 (2001).
46. Thorsen, T., Maerkl, S. J. & Quake, S. R. Microfluidic large-scale integration. *Science* **298**, 580–584 (2002).
47. Balagaddé, F. K., You, L., Hansen, C. L., Arnold, F. H. & Quake, S. R. Long-term monitoring of bacteria undergoing programmed population control in a microchemostat. *Science* **309**, 137–140 (2005).
48. Marcus, J. S., Anderson, W. F. & Quake, S. R. Microfluidic single-cell mRNA isolation and analysis. *Anal. Chem.* **78**, 3084–3089 (2006).
49. Maerkl, S. J. & Quake, S. R. A systems approach to measuring the binding energy landscapes of transcription factors. *Science* **315**, 233–237 (2007).
50. Fu, A. Y., Spence, C., Scherer, A., Arnold, F. H. & Quake, S. R. A microfabricated fluorescence-activated cell sorter. *Nature Biotech.* **17**, 1109–1111 (1999).
51. Li, P. C. H. & Harrison, D. J. Transport, manipulation, and reaction of biological cells on-chip using electrokinetic effects. *Anal. Chem.* **69**, 1564–1568 (1997).
52. Fu, A. Y., Chou, H. P., Spence, C., Arnold, F. H. & Quake, S. R. An integrated microfabricated cell sorter. *Anal. Chem.* **74**, 2451–2457 (2002).
53. Prokop, A. *et al.* NanoLiterBioReactor: long-term mammalian cell culture at nanofabricated scale. *Biomed. Microdevices* **6**, 325–339 (2004).
54. Groisman, A. *et al.* A microfluidic chemostat for experiments with bacterial and yeast cells. *Nature Methods* **2**, 685–689 (2005).
55. Cookson, S., Ostroff, N., Pang, W. L., Volfsong, D. & Hasty, J. Monitoring dynamics of single-cell gene expression over multiple cell cycles. *Mol. Syst. Biol.* **1**, 2005.0024 (2005).
56. Ryley, J. & Pereira-Smith, O. M. Microfluidics device for single cell gene expression analysis in *Saccharomyces cerevisiae*. *Yeast* **23**, 1065–1073 (2006).
57. Cai, L., Friedman, N. & Xie, X. S. Stochastic protein expression in individual cells at the single molecule level. *Nature* **440**, 358–362 (2006).
58. Di Carlo, D., Aghdam, N. & Lee, L. P. Single-cell enzyme concentrations, kinetics, and inhibition analysis using high-density hydrodynamic cell isolation arrays. *Anal. Chem.* **78**, 4925–4930 (2006).
59. Jeon, N. L. *et al.* Generation of solution and surface gradients using microfluidic systems. *Langmuir* **16**, 8311–8316 (2000).
60. **This was one of the first investigations to use a microfluidic device capable of generating spatial chemical gradients to study a biological phenomenon.**
61. Dertinger, S. K. W., Chiu, D. T., Jeon, N. L. & Whitesides, G. M. Generation of gradients having complex shapes using microfluidic networks. *Anal. Chem.* **73**, 1240–1246 (2001).
62. Jeon, N. L. *et al.* Neutrophil chemotaxis in linear and complex gradients of interleukin-8 formed in a microfabricated device. *Nature Biotech.* **20**, 826–830 (2002).
63. Mettetal, J. T., Muzzey, D., Gomez-Uribe, C. & van Oudenaarden, A. The frequency dependence of osmo-adaptation in *Saccharomyces cerevisiae*. *Science* **319**, 482–484 (2008).
64. Hersen, P., McClean, M. N., Mahadevan, L. & Ramanathan, S. Signal processing by the HOG MAP kinase pathway. *Proc. Natl Acad. Sci. USA* **105**, 7165–7170 (2008).
65. Bennett, M. R. *et al.* Metabolic gene regulation in a dynamically changing environment. *Nature* **454**, 1119–1122 (2008).
66. **References 33 and 58–60 are seminal studies that used microfluidic devices to create temporal changes in the growth medium to study dynamic biological phenomena.**
67. Siegal-Gaskins, D. & Crosson, S. Tightly regulated and heritable division control in single bacterial cells. *Biophys. J.* **95**, 2063–2072 (2008).
68. McKnight, T. E. *et al.* Intracellular integration of synthetic nanostructures with viable cells for controlled biochemical manipulation. *Nanotechnology* **14**, 551–556 (2003).
69. Balaban, N. O., Merrin, J., Chait, R., Kowalik, L. & Leibler, S. Bacterial persistence as a phenotypic switch. *Science* **305**, 1622–1625 (2004).
70. Gefen, O., Gabay, C., Mumcuoglu, M., Engel, G. & Balaban, N. O. Single-cell protein induction dynamics reveals a period of vulnerability to antibiotics in persister bacteria. *Proc. Natl Acad. Sci. USA* **105**, 6145–6149 (2008).
71. Heo, J., Thomas, K. J., Seong, G. H. & Crooks, R. M. A microfluidic bioreactor based on hydrogel-entrapped *E. coli*: cell viability, lysis, and intracellular enzyme reactions. *Anal. Chem.* **75**, 22–26 (2003).
72. Zhang, Z. *et al.* Microchemostat–microbial continuous culture in a polymer-based, instrumented microbioreactor. *Lab Chip* **6**, 906–913 (2006).

67. Peng, X. Y. & Li, P. C. A three-dimensional flow control concept for single-cell experiments on a microchip. 1. Cell selection, cell retention, cell culture, cell balancing, and cell scanning. *Anal. Chem.* **76**, 5273–5281 (2004).
68. Schmitz, C. H. J., Rowat, A. C., Koster, S. & Weitz, D. A. Drops: a picoliter array in a microfluidic device. *Lab Chip* **9**, 44–49 (2009).
69. Park, M. C., Hur, J. Y., Kwon, K. W., Park, S. H. & Suh, K. Y. Pumpless, selective docking of yeast cells inside a microfluidic channel induced by receding meniscus. *Lab Chip* **6**, 988–994 (2006).
70. Yun, K. S. & Yoon, E. Micro/nanofluidic device for single-cell-based assay. *Biomed. Microdevices* **7**, 35–40 (2005).
71. Wheeler, A. R. *et al.* Microfluidic device for single-cell analysis. *Anal. Chem.* **75**, 3581–3586 (2003).
72. Thompson, D. M. *et al.* Dynamic gene expression profiling using a microfabricated living cell array. *Anal. Chem.* **76**, 4098–4103 (2004).
73. Lu, H. *et al.* Microfluidic shear devices for quantitative analysis of cell adhesion. *Anal. Chem.* **76**, 5257–5264 (2004).
74. King, K. R. *et al.* A high-throughput microfluidic real-time gene expression living cell array. *Lab Chip* **7**, 77–85 (2007).
75. Volfson, D., Cookson, S., Hasty, J. & Tsimring, L. S. Biomechanical ordering of dense cell populations. *Proc. Natl Acad. Sci. USA* **105**, 15346–15351 (2008).
76. Cho, H. *et al.* Self-organization in high-density bacterial colonies: efficient crowd control. *PLoS Biol.* **5**, e302 (2007).
77. Hao, N. *et al.* Regulation of cell signaling dynamics by the protein kinase-scaffold Ste5. *Mol. Cell* **30**, 649–656 (2008).
78. Mao, H., Yang, T. & Cremer, P. S. A microfluidic device with a linear temperature gradient for parallel and combinatorial measurements. *J. Am. Chem. Soc.* **124**, 4432–4435 (2002).
79. Holden, M. A., Kumar, S., Castellana, E. T., Beskok, A. & Cremer, P. S. Generating fixed concentration arrays in a microfluidic device. *Sens. Actuators B Chem.* **92**, 199–207 (2003).
80. Zhu, X. *et al.* Arrays of horizontally-oriented mini-reservoirs generate steady microfluidic flows for continuous perfusion cell culture and gradient generation. *Analyst* **129**, 1026–1031 (2004).
81. Walker, G. M., Ozers, M. S. & Beebe, D. J. Cell infection within a microfluidic device using virus gradients. *Sens. Actuators B Chem.* **98**, 347–355 (2004).
82. Jiang, X. *et al.* A general method for patterning gradients of biomolecules on surfaces using microfluidic networks. *Anal. Chem.* **77**, 2338–2347 (2005).
83. Irimia, D., Geba, D. A. & Toner, M. Universal microfluidic gradient generator. *Anal. Chem.* **78**, 3472–3477 (2006).
84. Mao, H., Cremer, P. S. & Manson, M. D. A sensitive, versatile microfluidic assay for bacterial chemotaxis. *Proc. Natl Acad. Sci. USA* **100**, 5449–5454 (2003).
85. Diao, J. *et al.* A three-channel microfluidic device for generating static linear gradients and its application to the quantitative analysis of bacterial chemotaxis. *Lab Chip* **6**, 381–388 (2006).
86. Lin, F. & Butcher, E. C. T cell chemotaxis in a simple microfluidic device. *Lab Chip* **6**, 1462–1469 (2006).
87. Chung, B. G. *et al.* Human neural stem cell growth and differentiation in a gradient-generating microfluidic device. *Lab Chip* **5**, 401–406 (2005).
88. Paliwal, S. *et al.* MAPK-mediated bimodal gene expression and adaptive gradient sensing in yeast. *Nature* **446**, 46–51 (2007).
89. Lin, F. *et al.* Generation of dynamic temporal and spatial concentration gradients using microfluidic devices. *Lab Chip* **4**, 164–167 (2004).
90. Irimia, D. *et al.* Microfluidic system for measuring neutrophil migratory responses to fast switches of chemical gradients. *Lab Chip* **6**, 191–198 (2006).
91. Ingolia, N. T. & Weissman, J. S. Systems biology — reverse engineering the cell. *Nature* **454**, 1059–1062 (2008).
92. Tourovskaia, A., Figueroa-Masot, X. & Folch, A. Differentiation-on-a-chip: a microfluidic platform for long-term cell culture studies. *Lab Chip* **5**, 14–19 (2005).
93. Olofsson, J. *et al.* A chemical waveform synthesizer. *Proc. Natl Acad. Sci. USA* **102**, 8097–8102 (2005).
94. Lee, P. J., Gaige, T. A. & Hung, P. J. Dynamic cell culture: a microfluidic function generator for live cell microscopy. *Lab Chip* **9**, 164–166 (2009).
95. Zhang, X. & Roper, M. G. Microfluidic perfusion system for automated delivery of temporal gradients to islets of Langerhans. *Anal. Chem.* **81**, 1162–1168 (2009).
96. Charvin, G., Cross, F. R. & Siggia, E. D. Forced periodic expression of G<sub>1</sub> cyclins phase-locks the budding yeast cell cycle. *Proc. Natl Acad. Sci. USA* **106**, 6632–6637 (2009).
97. Chen, D. *et al.* The chemistrode: a droplet-based microfluidic device for stimulation and recording with high temporal, spatial, and chemical resolution. *Proc. Natl Acad. Sci. USA* **105**, 16843–16848 (2008).
98. King, K. R., Wang, S., Jayaraman, A., Yarmush, M. L. & Toner, M. Microfluidic flow-encoded switching for parallel control of dynamic cellular microenvironments. *Lab Chip* **8**, 107–116 (2008).
99. Taylor, R. J. *et al.* Dynamic analysis of MAPK signaling using a high-throughput microfluidic single-cell imaging platform. *Proc. Natl Acad. Sci. USA* **106**, 3758–3763 (2009).
100. Higgins, J. M., Eddington, D. T., Bhatia, S. N. & Mahadevan, L. Sickle cell vasoocclusion and rescue in a microfluidic device. *Proc. Natl Acad. Sci. USA* **104**, 20496–20500 (2007).
101. Polinkovsky, M., Gutierrez, E., Levchenko, A. & Groisman, A. Fine temporal control of the medium gas content and acidity and on-chip generation of series of oxygen concentrations for cell cultures. *Lab Chip* **9**, 1075–1084 (2009).
102. Breslauer, D. N., Lee, P. J. & Lee, L. P. Microfluidics-based systems biology. *Mol. Biosyst.* **2**, 97–112 (2006).
103. Kim, H. J., Boedicker, J. Q., Choi, J. W. & Ismagilov, R. F. Defined spatial structure stabilizes a synthetic multispecies bacterial community. *Proc. Natl Acad. Sci. USA* **105**, 18188–18193 (2008).
104. Keymer, J. E., Galajda, P., Muldoon, C., Park, S. & Austin, R. H. Bacterial metapopulations in nanofabricated landscapes. *Proc. Natl Acad. Sci. USA* **103**, 17290–17295 (2006).
105. Keymer, J. E., Galajda, P., Lambert, G., Liao, D. & Austin, R. H. Computation of mutual fitness by competing bacteria. *Proc. Natl Acad. Sci. USA* **105**, 20269–20273 (2008).
106. Miller, M. B. & Bassler, B. L. Quorum sensing in bacteria. *Annu. Rev. Microbiol.* **55**, 165–199 (2001).
107. Lucchetta, E. M., Lee, J. H., Fu, L. A., Patel, N. H. & Ismagilov, R. F. Dynamics of *Drosophila* embryonic patterning network perturbed in space and time using microfluidics. *Nature* **434**, 1134–1138 (2005).
108. Cai, L., Dalal, C. K. & Elowitz, M. B. Frequency-modulated nuclear localization bursts coordinate gene regulation. *Nature* **455**, 485–490 (2008).
109. De Jong, H. Modeling and simulation of genetic regulatory systems: a literature review. *J. Comput. Biol.* **9**, 67–103 (2002).
110. Glass, L. & Kauffman, S. A. The logical analysis of continuous, non-linear biochemical control networks. *J. Theor. Biol.* **39**, 103–129 (1973).
111. Savageau, M. A. Comparison of classical and autogenous systems of regulation in inducible operons. *Nature* **252**, 546–549 (1974).
112. Mather, W., Bennett, M. R., Hasty, J. & Tsimring, L. S. Delay-induced degrade-and-fire oscillations in small genetic circuits. *Phys. Rev. Lett.* **102**, 068105 (2009).
113. Tran, L. M., Rizk, M. L. & Liao, J. C. Ensemble modeling of metabolic networks. *Biophys. J.* **95**, 5606–5617 (2008).
114. Kepler, T. B. & Elston, T. C. Stochasticity in transcriptional regulation: origins, consequences, and mathematical representations. *Biophys. J.* **81**, 3116–3136 (2001).
- References 109–111 and 114 discuss some of the best modeling techniques that are common to both systems and synthetic biology, especially those that model the dynamics and stochasticity of gene regulation.**
115. Alon, U. *An Introduction to Systems Biology* (Chapman and Hall/CRC, Boca Raton, 2007).
116. Zamir, E. & Bastiaens, P. I. Reverse engineering intracellular biochemical networks. *Nature Chem. Biol.* **4**, 643–647 (2008).
117. Hasty, J., Isaacs, F., Dolnik, M., McMillen, D. & Collins, J. J. Designer gene networks: towards fundamental cellular control. *Chaos* **11**, 207–220 (2001).
118. Rao, C. V. & Arkin, A. P. Stochastic chemical kinetics and the quasi-steady-state assumption: application to the Gillespie algorithm. *J. Chem. Phys.* **118**, 4999–5010 (2003).
119. Gillespie, D. T. Exact stochastic simulation of coupled chemical-reactions. *J. Phys. Chem.* **81**, 2340–2361 (1977).
- This paper describes the Gillespie algorithm, which is used to simulate systems of randomly interacting chemical species and is now ubiquitously used in the synthetic biology community.**
120. Volfson, D. *et al.* Origins of extrinsic variability in eukaryotic gene expression. *Nature* **439**, 861–864 (2006).
121. MacDonald, N. Time lag in a model of a biochemical reaction sequence with end product inhibition. *J. Theor. Biol.* **67**, 549–556 (1977).
122. Mahaffy, J. M. & Pao, C. V. Models of genetic control by repression with time delays and spatial effects. *J. Math. Biol.* **20**, 39–57 (1984).
123. McAdams, H. H. & Shapiro, L. Circuit simulation of genetic networks. *Science* **269**, 650–656 (1995).
124. Bratsun, D., Volfson, D., Tsimring, L. S. & Hasty, J. Delay-induced stochastic oscillations in gene regulation. *Proc. Natl Acad. Sci. USA* **102**, 14593–14598 (2005).
125. Budschuh, R., Hayot, F. & Jayaprakash, C. Fluctuations and slow variables in genetic networks. *Biophys. J.* **84**, 1606–1615 (2003).
126. Bennett, M. R., Volfson, D., Tsimring, L. & Hasty, J. Transient dynamics of genetic regulatory networks. *Biophys. J.* **92**, 3501–3512 (2007).
127. Gardner, T. S., Cantor, C. R. & Collins, J. J. Construction of a genetic toggle switch in *Escherichia coli*. *Nature* **403**, 339–342 (2000).
128. Elowitz, M. B. & Leibler, S. A synthetic oscillatory network of transcriptional regulators. *Nature* **403**, 335–338 (2000).
- References 127 and 128 are two of the earliest triumphs of synthetic biology, the construction of a genetic toggle switch and a synthetic oscillator, respectively.**

### Acknowledgements

We would like to thank O. Mondragon and S. Cookson for initial literature searches, and B. Baumgartner for thorough readings of the drafts. This work was supported by the National Institute of General Medical Sciences of the National Institutes of Health (GMO79333).

### DATABASES

Entrez Gene: <http://www.ncbi.nlm.nih.gov/entrez/query.fcgi?db=gene>  
 GAL1 | GAL3  
 UniProtKB: <http://www.uniprot.org>  
 Crz1 | Fus3 | Gfp | Kss1 | Ste5  
 FlyBase: <http://www.flybase.org>  
 even-skipped

### FURTHER INFORMATION

Mathew R. Bennett's homepage: <http://www.bioc.rice.edu/~mb24>  
 Jeff Hasty's homepage: <http://biodynamics.ucsd.edu>

ALL LINKS ARE ACTIVE IN THE ONLINE PDF